Molecular Dynamics Revealed from Frequency Dependent Heat Capacity

Christoph Schick[a*], Andreas Wurm[a], Mikhail Merzlyakov[a], Alexander Minakov[b], Hervé Marand[c]

[a] University of Rostock, Dept. Physics, Universitätsplatz 3, 18051 Rostock, Germany, e-mail: christoph.schick@physik.uni-rostock.de
[b] General Physics Institute, RAS, Vavilov st. 38, 117942 Moscow, Russia
[c] VPI & SU, Dept. of Chemistry, Blacksburg, VA 24061-0212, USA

SUMMARY: Temperature modulated DSC (TMDSC) measurements at reasonably high frequencies allow for the determination of baseline heat capacity. In this particular case vitrification and devitrification of the rigid amorphous fraction (RAF) can be directly observed. 0.01 Hz seems to be a reasonably high frequency for Bisphenol-A Polycarbonate (PC). The RAF of PC is established during isothermal crystallization. Devitrification of the RAF seems to be related to the pre-melting peak. For PC the melting of small crystals between the lamellae is thought to yield the pre-melting peak.

Introduction

From glass transition it is well known and generally accepted that heat capacity can be described by complex numbers. The typical frequency dependence like for other relaxation processes can be observed – a sigmoidal step in real and a peak in imaginary part of heat capacity [1-3]. At given temperature the peak frequency ω can be related to the mean relaxation time τ according to $\omega \cdot \tau = 1$.

Recent measurements also indicate a frequency dependence of the heat capacity of semicrystalline polymers outside the glass transition range [4, 5]. These observations are related to the occurrence of an excess heat capacity that can be observed in a rather wide temperature range between the glass transition and the melting temperature. The origin of this excess heat capacity and its frequency dependence are not yet understood. Probably the molecular processes involved are related to the surface of the polymer crystallites and often the term reversible melting [6] is used. For polymers showing a sliding diffusion (α relaxation) in the crystallites, large contributions to reversible melting are probably due to

 CCC 1022-1360/00/$ 17.50+.50/0

surface melting [7]. For other semicrystalline polymers we do not know which surfaces, growth or fold, are responsible for the process of reversible melting and the corresponding excess heat capacity.

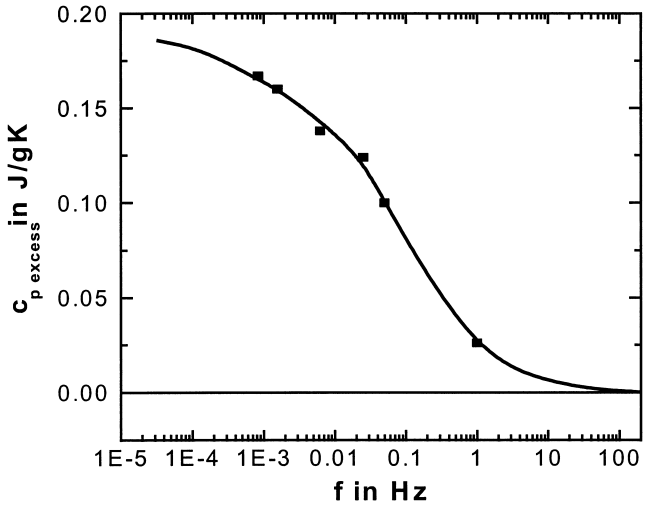

Fig. 1: Excess-heat capacity of PCL after 2000 minutes crystallization at 328 K as a function of modulation frequency [4]. PerkinElmer Pyris 1 DSC and AC calorimeter [8].

In order to obtain information about the characteristic time scale of the molecular processes related to excess heat capacity we have studied the frequency dependence of complex heat capacity during quasi-isothermal crystallization. To extend the frequency range available with TMDSC (10^{-5} Hz - 10^{-1} Hz) AC calorimetric measurements were performed at frequency 1 Hz. A mean relaxation time in the order of seconds can be estimated for the process at 328 K for PCL. As can be seen from fig. 1 the frequency range available is still not broad enough for a detailed discussion of the curve shape. From this curve one expects for frequencies higher than about 10 Hz to measure baseline heat capacity without contributions due to reversible melting. Baseline heat capacity means that part of heat capacity due to vibrations etc. In other words it is the heat capacity without any contribution from latent heat. In this paper we will focus on baseline heat capacity which can be measured at the high frequency limit, see fig. 1. In this case vitrification and devitrification of the rigid amorphous fraction (RAF) of semicrystalline polymers can be studied.

There are two possible paths to reach this goal: To extend the frequency range of heat capacity measurements or to study a polymer with very slow dynamics of the reversible melting so that the high frequency limit is reached at standard frequencies of temperature modulated DSC

(TMDSC). For PCL, as an example, frequencies above 100 Hz are necessary to measure baseline heat capacity. This is far above the TMDSC high frequency limit of 0.1 Hz. A chance to reach such a high frequency for heat capacity measurements is given with recent developments of AC calorimetry [8] rather than by the 3ω-method [2] where it seems to be difficult to distinguish between heat capacity and thermal conductivity contributions. In this paper we followed the second approach and have studied Bisphenol-A Polycarbonate (PC). PC was chosen for this study because of its very slow crystallization behavior [9].

Experimental Part

TMDSC, a technique described for the first time in 1971 by Gobrecht et al. [1], and the necessary data treatments are described elsewhere [1, 10-14]. If one wants to perform TMDSC measurements in a broad frequency range high sensitive DSC apparatuses with different time constants like PerkinElmer Pyris 1 DSC and Setaram DSC 121 must be used, for details see [15]. For measurements at a fixed frequency of 0.01 Hz a TA Instruments DSC 2920CE was used. For the comparison of various experimental data sets a careful temperature calibration of all instruments is necessary. The DSC's are calibrated at zero heating rate according to the GEFTA recommendation [16]. The calibration was checked in TMDSC mode with the smectic A to nematic transition of 8OCB [17, 18].

The polycaprolactone (PCL) is a commercial sample synthesized by Aldrich Chemie with a molecular weight average M_W = 55,700 g/mol. More details about the sample are reported in [19]. The Bisphenol-A Polycarbonate was obtained from General Electric (tradename LEXAN™) and was purified by dissolution in chloroform, filtering and precipitation in methanol [20, 21]. The weight average molar mass and polydispersity index for the polycarbonate were obtained by Gel Permeation Chromatography in chloroform (M_w = 28,400 g/mol and M_w/M_n = 2.04). The heat capacity data for these polymers in the liquid and the solid state are available from ATHAS data bank [22].

Results and Discussion

In a first approximation the expected baseline heat capacity c_{pb} for the semicrystalline sample can be calculated using a simple two-phase model according to

$$c_{pb}(T,t) = \chi_c(T,t)\, c_{p\,crystal}(T) + (1-\chi_c(T,t))\, c_{p\,melt}(T) \qquad (1)$$

with $c_{p\ crystal}$ specific heat capacity for the crystal, $c_{p\ melt}$ that for the melt and χ_c degree of crystallinity. For most polymers deviations from such a simple two-phase model are observed [23, 24]. Introducing a rigid amorphous fraction the baseline heat capacity can be obtained from

$$c_{pb}(T,t) = \chi_r(T,t)\, c_{p\ rigid}(T) + (1-\chi_r(T,t))\, c_{p\ melt}(T) \qquad (2)$$

with $c_{p\ rigid}$ specific heat capacity of the rigid fraction that contains crystalline and rigid (immobilized, vitrified) amorphous material (RAF). For most polymers $c_{p\ rigid}$ equals $c_{p\ crystal}$ and is available from [22]. $\chi_r(T,t)$ is the rigid fraction. At the glass transition temperature $\chi_r(T_g)$ can be obtained from the step of heat capacity at T_g.

$$\chi_r = 1 - \frac{\Delta c_p}{\Delta c_{pa}} \qquad (3)$$

where Δc_p is the heat capacity step of the semicrystalline sample while Δc_{pa} is that of the totally amorphous sample. To obtain the exact baseline heat capacity in the temperature range between glass transition and melt iterative procedures are necessary [25, 26].

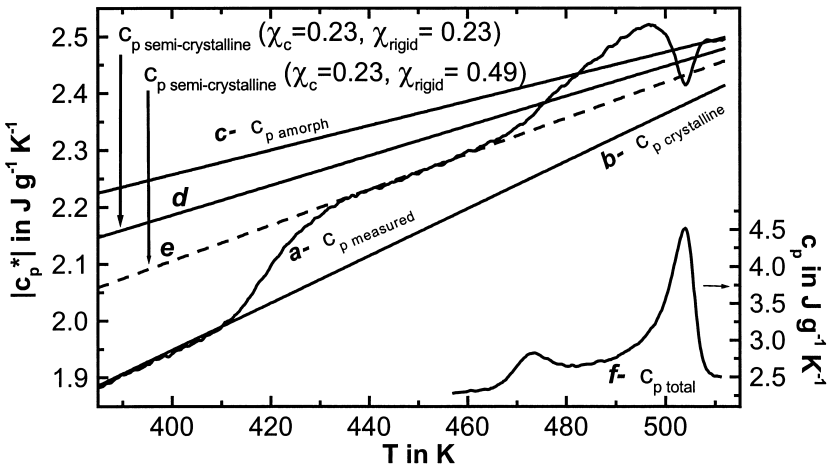

Fig. 2: TMDSC scan measurement of semicrystalline PC at underlying heating rate 0.5 K/min, temperature amplitude 0.5 K and period 100 s, curve a. Curve b and c correspond to heat capacities from ATHAS data bank for crystalline and liquid PC, respectively. Curve d was estimated from a two phase model, eq. (1) and curve e from a three phase model, eq. (2) using data from T_g. Curve f shows the total heat capacity in the melting region. TA Instruments DSC 2920CE .

The modulus of complex heat capacity and the total heat flow from a TMDSC heating scan of PC are shown in fig. 2. Curve **e** in fig. 2 was estimated, eq. (2), from the data obtained at the glass transition eq. (3). Outside the melting region this can be used as the baseline heat capacity. For PC this is approximately true above glass transition and below 460 K. Measured heat capacity equals this value as can be seen in fig. 2. This shows that there is no reversible melting and no excess heat capacity on the time scale of 100 s.

Because the maximum crystallization rate of PC is observed at ca. 460 K there is a chance to study crystallization of PC without any excess heat capacity at 0.01 Hz.

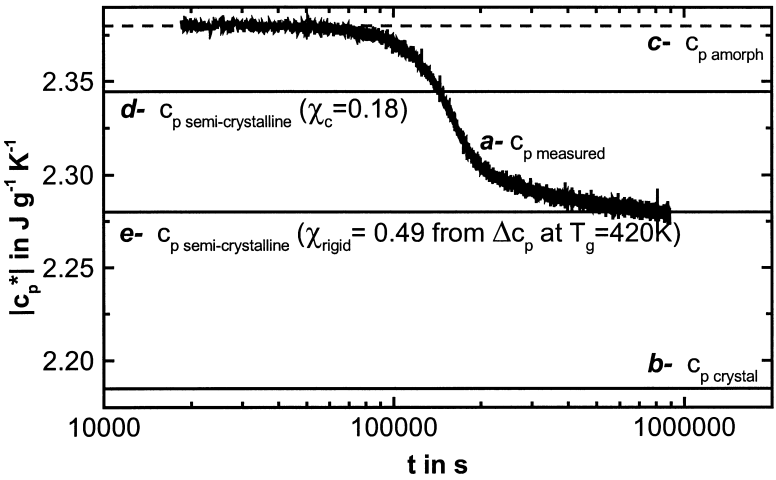

Fig. 3: Time evolution of heat capacity during quasi-isothermal crystallization of PC at 456.8 K, curve ***a***. Curve ***b*** and ***c*** correspond to crystalline and liquid heat capacities from ATHAS data bank, respectively. Curve ***d*** was estimated from a two phase model, eq. (1) and curve ***e*** from a three phase model, eq. (2).

In fig. 3 the time evolution of heat capacity during isothermal crystallization of PC at 456.8 K is shown. Measured heat capacity becomes smaller than baseline heat capacity obtained from eq. (1), curve ***d***, – indicating the occurrence of a significant RAF during the crystallization process. After 10^6 s (ca. 11 days) the heat capacity equals baseline heat capacity according to eq. (3), curve ***e***, using the data for the RAF from the step of heat capacity at the glass transition at 420 K. From this observation we can conclude that the total RAF of PC is established (vitrified) during the isothermal crystallization and no additional vitrification

occurs during cooling to the glass transition temperature. The question arises at what temperature the RAF devitrifies on heating – before the crystals melts or is devitrification of the RAF part of the main melting. The heat capacity measured at scanning through the melting region of PC, fig. 2 curve ***a***, shows some excess heat capacity in the temperature range 460 K – 510 K due to reorganization on slow heating (0.5 K/min). To measure heat capacity without contributions from reorganization quasi-isothermal TMDSC measurements at stepwise increasing temperatures were performed. The results in the temperature range above glass transition, see fig. 2, are shown in fig. 4.

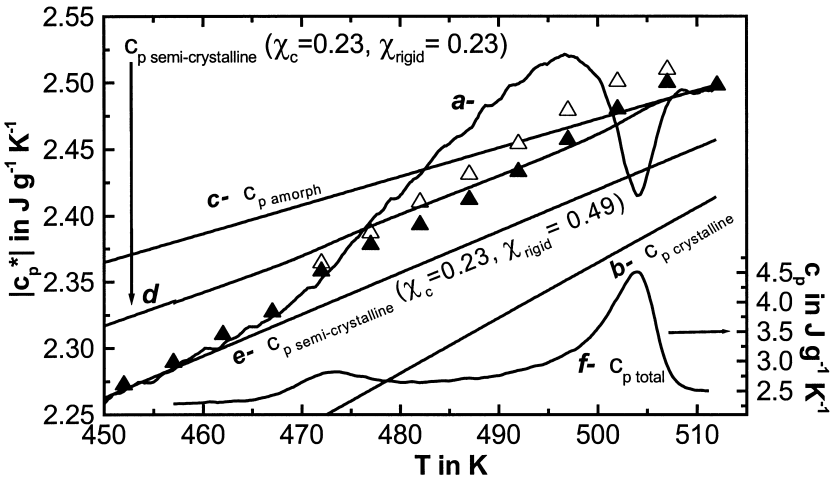

Fig. 4: Magnified part of fig. 1 in the melting region of PC. Curves as in fig. 1 except curve ***d*** where now the changes in crystallinity in the main melting region are taken into account. The triangles show the heat capacities from quasi-isothermal TMDSC measurements on stepwise increasing temperatures. The data were taken after 15 minutes, open triangles, and after 3 hours, solid triangles.

From about 470 K changes in heat capacity during the quasi-isothermal measurements can be seen. The difference between open and solid triangles corresponds to 3 hours. After 3 hours, solid triangles, the sample has stabilized, except in the temperature range 490 K – 505 K where re-crystallization occurs. Let us focus on the region of the pre-melting peak between 460 K - 485 K. A step-like increase of heat capacity can be observed. The heat capacity starts

to deviate from the baseline heat capacity obtained from a three-phase model including RAF, eq. (2) curve ***e***, and around 480 K it is close to the baseline heat capacity obtained from a two phase model, eq. (1) curve ***d***. In eq. (1) only crystalline and mobile amorphous material are taken into account. At higher temperatures, during main melting, heat capacity approximately follows increasing baseline heat capacity as estimated from the temperature dependent crystallinity and eq. (1), curve ***d***, and finally reach the liquid heat capacity, curve ***c***.

Conclusion

TMDSC heat capacity measurements in the high frequency limit allow to measure baseline heat capacity as probably shown on the example of PC. For PC the RAF is established during isothermal crystallization as can be seen from fig. 3. Devitrification of the RAF seems to be related to the pre-melting peak or lowest endotherm, see fig. 4. For PC the melting of small crystals between the lamellae yield the pre-melting peak [9, 20, 21, 27]. The immobilization of the amorphous material around these small crystals, which are formed during isothermal crystallization [27], results in the vitrification of the RAF during crystallization and in its devitrification during melting. From fig. 4 a remaining RAF of about 10% can be estimated from the small difference between measured and baseline heat capacity. This RAF may be at the fold surface of the lamellae.

Acknowledgement

This research was supported by the European Commission (grant IC15CT96-0821), the German Science Foundation (grant DFG Schi-331/5-1) and the government of Mecklenburg-Vorpommern. Support by PerkinElmer Instruments and TA Instruments is acknowledged.

References

1. H. Gobrecht, K. Hamann, G. Willers, *Journal of Physics E: Scientific Instruments* **4,** 21 (1971)
2. N. O. Birge, S. R. Nagel, *Phys. Rev. Lett.* **54,** 2674 (1985)
3. S. Weyer, A. Hensel, C. Schick, *Thermochim. Acta* **304/305,** 251 (1997)
4. C. Schick, M. Merzlyakov, A. Minakov, A. Wurm, *J. Therm. Anal. Cal.* **59,** 279 (2000)
5. Y. Saruyama, *Thermochim. Acta* **330,** 101 (1999)
6. I. Okazaki, B. Wunderlich, *Macromol.* **30,** 1758 (1997)

7. W. Hu, T. Albrecht, G. Strobl, *Macromol.* **32,** 7548 (1999)
8. A.A. Minakov, Yu. Bugoslavsky, C. Schick, *Thermochim. Acta* **317,** 117 (1998)
9. S. Sohn, "Crystallization Behavior of Bisphenol A Polycarbonate: Effect of Time, Temperature and Molar Mass", Ph.D. Thesis, Virginia Polytechnic and State University, April 2000
10. B. Wunderlich, Y.M. Jin, A. Boller, *Thermochim. Acta,* **238,** 277 (1994)
11. M. Reading, *Trends Polym. Sci.,* **8,** 248 (1993)
12. J. E. K. Schawe, *Thermochim. Acta* **260,** 1 (1995)
13. M. Merzlyakov, C. Schick, *Thermochim. Acta* **330,** 55 and 65 (1999)
14. S. Weyer, A. Hensel, C. Schick, *Thermochim. Acta* **304/305,** 267 (1997)
15. M. Merzlyakov, A. Wurm, M. Zorzut, C. Schick, *J. Macromol. Sci.– Phys.* **38,** 1045 (1999)
16. S. M. Sarge, W. Hemminger, E. Gmelin, G. W. H. Höhne, H. K. Cammenga, W. Eysel, *J. Therm. Anal.* **49,** 1125 (1997)
17. A. Hensel, C. Schick, *Thermochim. Acta* **304/305,** 229 (1997)
18. C. Schick, U. Jonsson, T. Vassiliev, A. Minakov, J. Schawe, R. Scherrenberg, D. Lörinczy, *Thermochim. Acta* **347,** 53 (2000)
19. P. Skoglund, A. Fransson, *J. Appl. Polym. Sci.* **61,** 2455 (1996)
20. S. Sohn, A. Alizadeh, H. Marand, *Polymer* **41(24)**, 000 (2000)
21. A. Alizadeh, S. Sohn, J. Quinn, H. Marand, L. Shank, H.D. Iler, *Macromolecules*, submitted (May 2000).
22. B. Wunderlich, *Pure & Appl. Chem.* **67,** 1019 (1995); see on WWW URL: http://web.utk.edu/~athas/databank/intro.html.
23. Y. Ishida, K. Yamafuji, H. Ito und M. Takayanagi, *Kolloid-Z. & Z. Polym.* **184,** 97 (1962)
24. H. Suzuki, J. Grebowicz, B. Wunderlich, *Makromol. Chem.* **186,** 1109 (1985)
25. V.B.F. Mathot, Ch. 5: 'Thermal Characterization of States of Matter' in 'Calorimetry and Thermal Analysis of Polymers', V.B.F. Mathot (Ed.); Hanser Publishers, München 1994
26. M. Alsleben, C. Schick, *Thermochim. Acta* **238,** 203 (1994)
27. H. Marand, A. Alizadeh, R. Farmer, R. Desai, V. Velikov *Macromolecules* **33**, 3392 (2000)